KINETICS OF PYROLYSIS AND COMBUSTION OF OIL SHALE SAMPLE FROM THERMOGRAVIMETRIC DATA

Shabbar Syed, **Rana Qudaih, Ilham Talab, Isam Janajreh.** *ijanajreh@masdar.ac.ae*, Mechanical Engineering Program, Masdar Institute of Science and Technology (MI), Abu Dhabi, UAE

1. ABSTRACT

Thermogravimetric (TG) data of oil shale obtained at MI (Waste to Energy laboratory) are studied to evaluate the kinetic parameters (i.e activation energy (E) and pre-exponential factor (A)) for El-Lujjun oil shale samples. Different heating rates simulating pyrolysis at constant flow rate of nitrogen (N_2) are employed with the maximum process temperature of ~800 ^oC. The extent of char combustion is found out by relating TG data for pyrolysis and combustion with the ultimate analysis. Due to distinct behavior of oil shale during pyrolysis, TG curves are divided into three separate events: moisture release; devolatization; and evolution of fixed carbon/char, where for each event, kinetic parameters, based on Arrhenius theory, are calculated. Three methods are used and compared: integral method; direct Arrhenius plot method; and temperature integral approximation method. Results showed that integral method is more close to the experiment.

Keywords: El-Lujjun, Oil shale, Gasification, Pyrolysis, Thermogravimetric (TG) analyses, Activation Energy, Pre-exponent factor, Arrhenius equation, Kinetic parameters.

2. INTRODUCTION

Increasing fuel prices, the eminent fear of the limited conventional energy resources, and the projected growth of heavy industry have placed great pressure on energy supplies. Oil shale is an abundant resource in USA, Australia, China, Jordan, Morocco, and Estonia and its energy extraction is under intensive research (Strizhakova and Usova 2008). Despite research efforts dedicated to the conversion of oil shale into synthetic motor fuels and to the chemical products, only few commercial projects are implemented, as summarized in Table 1.

High temperature devolatization plays an important role in the combustion and gasification of shale oil. Therefore it is necessary to develop models to predict the behavior of the feedstock when it is subjected to high temperature. The relationship between the extents of reaction as it proceeds with the temperature can be determined by Arrhenius equation. Activation energy (*E*) and pre-exponential factor (*A*) are the two important parameters in Arrhenius equation which are determined by thermal analysis. These parameters can be further used in numerical simulation models such as CFD to investigate the behavior of the feedstock under different operating conditions (Yu, Lu et al. ; Choi, Li et al. 2001; Watanabe and Otaka 2006).

Table 1: Main examples of oil shale retorting projects (Dyni)

Location	Capacity (t/d)	Technology	Product
Russia:		Vertical retorting with natural gas agent	Liquid fuel, chemicals and low calorific gas
Slantsy	100		
syzran	30		
Estonia:			
Narva	130		
Kivyili	100		
Kohtla-Jarve	1000/200/40		
Australia:		Horizontal retorting	Naphtha, light distillate fuel oil and high calorific gas
Stuart	6000		
Brazil:		Vertical retorting	Liquid fuel, naptha, sulfur, high calorific gas, coke
Sao Mateus do sul	6300/1500		
China:		Vertical Retorting	Liquid fuel, carbon, soot and low calorific gas
Fushun	100		

Thermogravimetric analysis (TGA) is extensively used to determine the global kinetic parameters of pyrolysis and combustion. TG analysis can be performed using both isothermal and non-isothermal techniques which have several advantages over the former.

Firstly, maintaining a constant heating rate is less demanding compared to retain a constant temperature environment during an experiment, especially when exothermic reactions are involved. Secondly, because of a known steady heating rate the experiment time is significantly reduced. Moreover, the working procedure of most of the operating oil shale reactors are based on a constant heating rate, therefore, non-isothermal analysis give results in close proximity to practical procedure.

There are mainly three procedures widely used to calculate the Arrhenius parameters from thermogravimetric data. (Coats and Redfern 1964) used data from thermogravimetric analysis to evaluate kinetic parameters of solid-state reaction of calcium oxalate monohydrate. This method involves the approximation of the temperature integral to a series of expansion which results in a series for an indefinite temperature integral. This method is widely used to evaluate the kinetic parameters for constant heating rate and it is extensively acknowledged (Rajeshwar 1981; Dollimore, Evans et al. 1992; Dogan and Uysal 1996; Leung and Wang 1998; Rao and Sharma 1998; Bockhorn, Hornung et al. 1999; Vyazovkin and Wight 1999; Kök and Pamir 2000; Williams and Ahmad 2000; Liu, Fan et al. 2002; Starink 2003; Capart, Khezami et al. 2004). Several other approximations are also used to make this method more viable. (Qing, Baizhong et al. 2007) showed that if an approximation is made that relates activation energy to temperature then Coats' model can be further simplified into to a single equation from which the E and A can be calculated.

The second method is commonly known as "Direct Arrhenius plot method". This method avoids the approximation for the temperature integral which is the major assumption of Coats kinetics(Coats and Redfern 1964) model. (Qing, Baizhong et al. 2007) used this method to calculate kinetics parameters for Huadian oil shale at different order of reaction. This method is fairly straightforward compared to the integral method. The only approximation is for the temperature differential of the mass fraction. In this work a linear approximation for temperature differential through DTG curve is used in conjunction with a unity order of reaction.

The temperature integral of Arrhenius equation cannot be analytically integrated. However, researcher such as (Madhusudanan, Krishnan et al. 1986) devised a new approximation for the temperature integral. This method uses a three-term function approximation which can be used to estimate the kinetic parameters from non-isothermal TG data. This method, because of its simplicity and workability, is commonly used in integral methods of thermal analysis (Obaid, Alyoubi et al. 2000; Diefallah, Gabal et al. 2001; Órfão and Martins 2002; Tang, Liu et al. 2003).

In this research, The TG analysis is performed on El-Lujjun oil shale samples and all the above mentioned methods are applied to calculate the Arrhenius parameters. The objective of this work is to analyze the oil shale samples using Simultaneous Thermal Analyzer SDT Q600 at four different heating rates and to calculate the kinetic parameters on the basis of experimental results. Due to fairly different behavior of oil shale after devolatization of the sample during pyrolysis, as discussed in proceeding session, the TG curve is divided into three events to calculate the kinetic parameters. The results of kinetic parameters are then used to simulate the TG curve by putting the value in respective Arrhenius model/methods. In this way the kinetic parameters are compared with the experimental TG curve. Also, a root mean square error is calculated for each method, which relates the accuracy of calculated results with the obtained TG experimental data.

3. EXPIREMNTAL SETUP

The oil shale samples used in this work were obtained from the El-Lujjin deposit in Jordan which were crushed, homogenized, ball milled and then sieved to 50μm size as depicted in Figure 1 (Q.Rana 2010). The TG analysis is based on the precise measurements of the mass change of the sample as a function of a specified temperature profile. The goal is to generate a high resolution of the sample decomposition and, if possible, a distinct event to each of the drying (moisture release), devolatization, evolution of fixed carbon/char and combustion processes.

At first, the equipment was calibrated using calcium oxalate and the results are shown in Figure 2. The weight of the samples used for pyrolysis of oil shale are in the range of 8-15 g, and that are subjected to heating rates of 5; 10; 15; and 20^{o}C/min. During pyrolysis, nitrogen gas is used at 100 ml/min till 800^{o}C when it is switched off. By employing different heating rates with high temperature guarantees to capture the three events during pyrolysis with accurate measurement of mass change.

Figure 1: Oil shale sample after milling and during the sieving

The result of TG analysis of oil shale samples during pyrolysis with constant heating rate are shown in Figure 3. The average moisture content in the oil shale sample is found to be 1.43%±0.2, it also contains 23.13%±0.5 of volatiles and 13.54%±0.38 of fixed carbon while ash constitute the balance.

The DTG plot, as shown in Figure 4, clearly illustrates the three stages of weight loss during pyrolysis. The first stage of moisture release, which corresponds to the release of water vapor from the mineral layer, ends during the pre-heating of sample around 280°C (±15°C). Then, the volatile hydrocarbons start evolving and continued up to 540°C (±10°C). Further increase in temperature leads to the formation of fixed carbon. It is evident from Figure 3 that the weight of char decreases exponentially. The sudden decrease of the weight, which is unexpected since char and minerals do not usually react under nitrogen conditions, poses the possibility of reactions i.e. combustion or gasification.

To explain this claim, a sample of Kentucky coal is pyrolized under nitrogen conditions in STA up to 1300°C, as shown in Figure 5. After devolatization at around 550°C, the Kentucky coal sample shows a relatively linear behavior of weight loss as compare to oil shale. This behavior of Kentucky coal is expected, as neither char nor minerals react with nitrogen gas. Therefore, char present in oil shale undertakes other reactions than carbon combustion which causes the further exponential weight loss of the sample. J.O.Jaber (Jaber and Probert 1999) explain this event by referring to the decomposition of carbonates i.e. calcite and dolomite, present in the sample. The high temperature attribute the thermal break down of carbonate into CO_2 which further reacts with the residual char, as described by the Boudouard reaction:

$$C + CO_2 \rightarrow 2CO$$

Assuming the weight loss is due to the above mentioned Boudouard reaction then the complete conversion of char into CO is dependent upon the quantity of CO_2 evolving from the sample. TG curve for oil shale, as shown in Figure 3, shows an average of 61.88% of ash present in the sample.

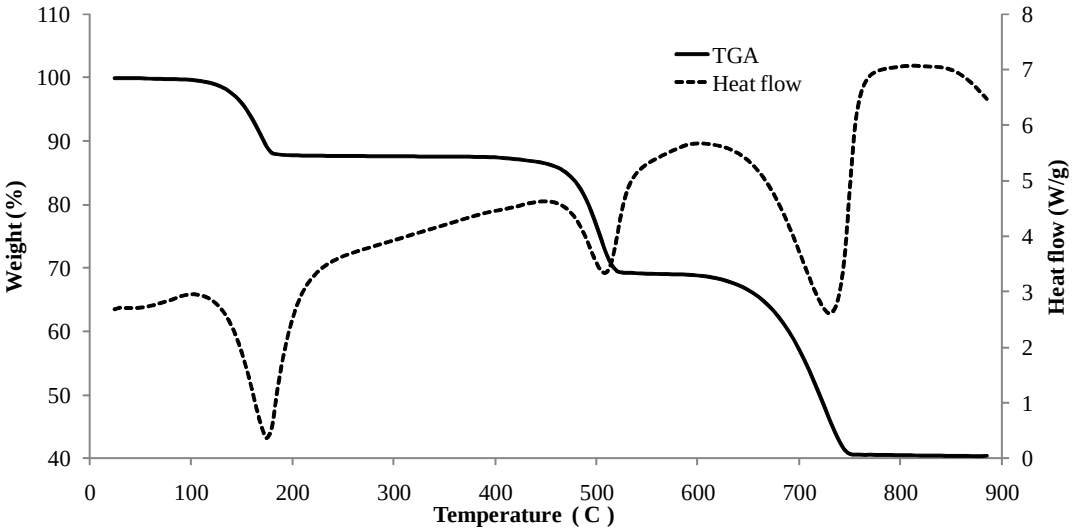

Figure 2: Pyrolysis of calcium oxalate at 20°C/min.

But this value is strongly dependent upon the extent of Boudouard reaction, Therefore, to estimate the actual amount of CO_2 present, ultimate analysis is carried out on oil shale sample. The average result of five tests are shown in Table 2 (Q.Rana 2010). It is clear from the ultimate analysis that the average amount of ash balance is 58.50%, which makes an ash difference of 3.38% as compare to TG analysis. Earlier is has been reported that the ash of oil shale contains a considerable amount of sulfur (Shawabkeh, Al-Harahsheh et al. 2004; Oja, Elenurm et al. 2007; Shawabkeh and Harahsheh 2007). So it can be concluded that the 3.38 % of sulfur, as reported in ultimate analysis, remains un-reacted during TG analysis. To analyze further, a sample of oil shale is combusted at a constant heating rate of 10 C/min. Initially the sample is heated in an inter nitrogen environment up to 600°C then a constant flow rate of air purging is used for combustion. The result of combustion, as shown in Figure 6, shows the mass balance of ash as 61.55. This amount of ash is in close proximity with the ash generated during pyrolysis, which supports the claim that sulfur remains unburnt during combustion. The ash balance during pyrolysis and combustion also reveal that the amount of CO_2 evolving during pyrolysis is enough to consume fixed carbon/char through Boudouard reaction. Additional behavior of oil shale combustion will be presented in future studies.

Table 2: Elemental composition of oil shale (Q.Rana 2010).

Element	Weight (%)
N	0.41
C	20.33
H	2.09
S	3.38
O	15.28
Mass balance (Ash)	58.5

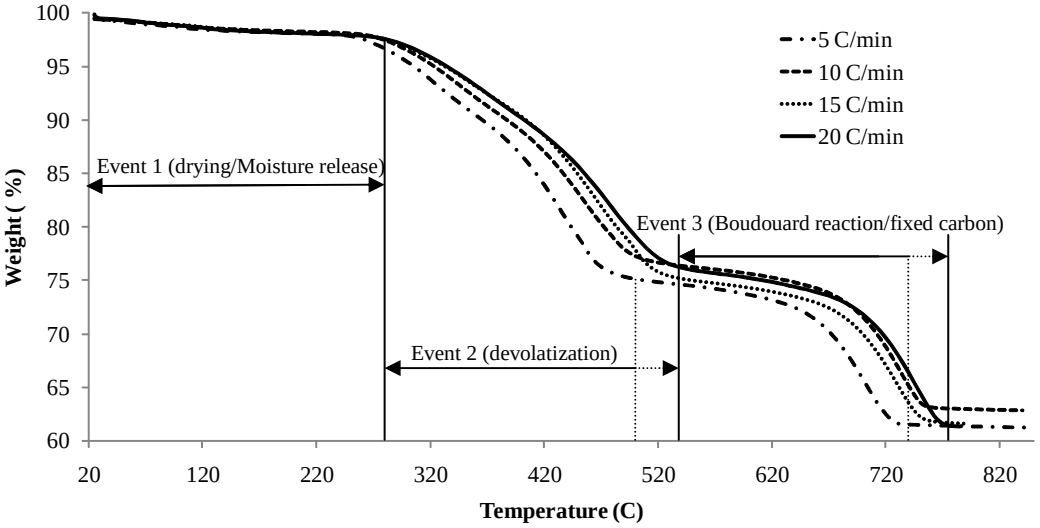

Figure 3: TGA for oil shale pyrolysis at different heating rates.

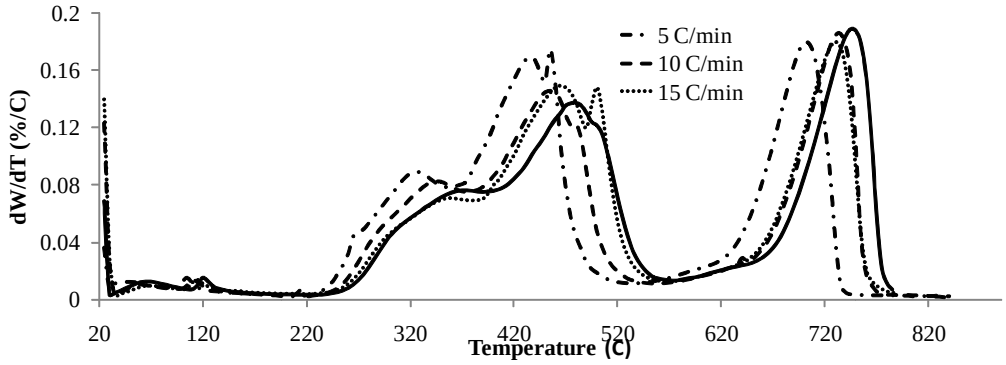

Figure 4: DTG plot for oil shale pyrolysis

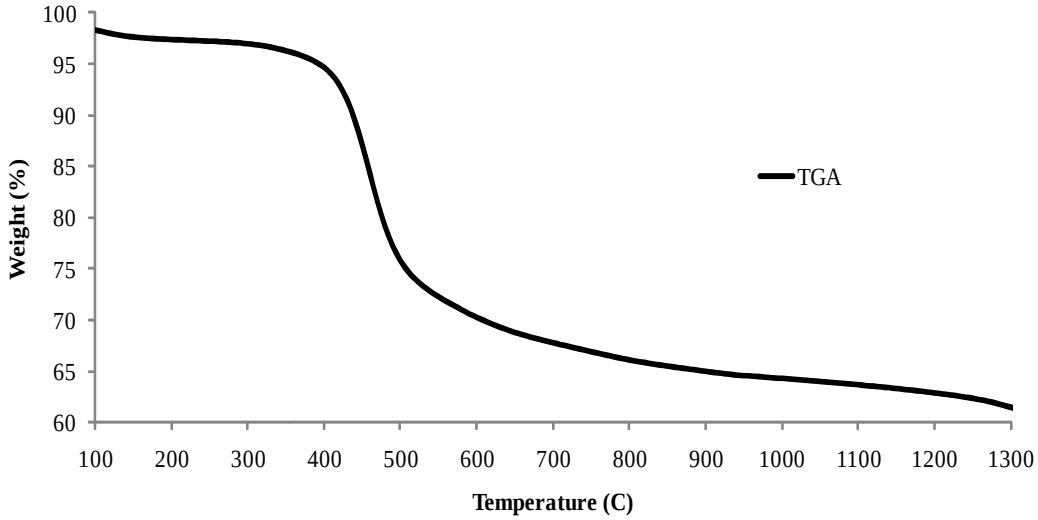

Figure 5: TGA for Kentucky coal pyrolysis at 15 C/min heating rates.

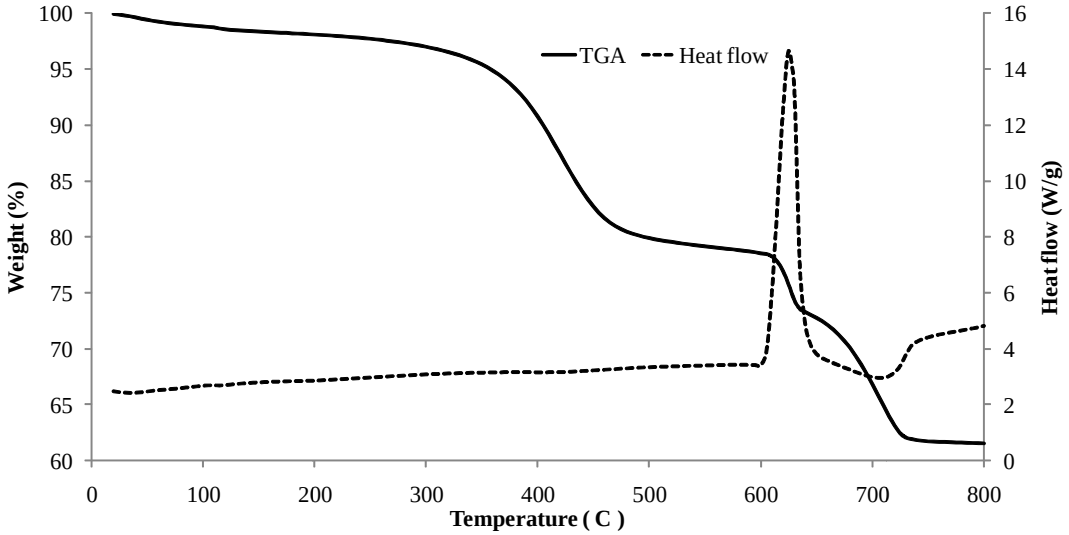

Figure 6: Combustion of oil shale at 10°C/min

4. KINETIC ANALYSIS

The organic material present in the oil shale is a solid substance and it is insoluble in water, called kerogen. The thermal decomposition of kerogen yields volatile materials in the form of gas, oil and solid char. (Thakur and Nuttall Jr 1987) shows the complete thermal decomposition of kerogen in two steps,

$Kerogen \rightarrow Bitumen + gas$

and then Bitumen further decomposes as in:

$Bitumen \rightarrow oil + gas + char$

Following the thermal decomposition of kerogen, each event during the pyrolysis of oil shale can be represented by the following equation,

$$\frac{dX}{dt} = K(1-X)^n \quad (1)$$

where X is the extent of conversion, t is the time, K is the specific rate constant and n is the order of reaction. The extent of conversion can be represented as follow,

$$X = \frac{X_0 - X_t}{X_0 - X_X} \quad (2)$$

where X_0 is the initial weight, X_X is the final weight and X_t is the weight at time t. The temperature dependence of the rate constant is given by Arrhenius equation:

$$K = Ae^{-\frac{E}{RT}} \quad (3)$$

where A is the pre-exponent factor, E is the activation energy, T is the temperature and R is the universal gas constant. To simplify the calculations, the order of reaction (n) is assumed unity. For constant heating rate (β), a linear relation between time and temperature can be written as,

$$\beta = \frac{dT}{dt} \tag{4}$$

Now, substituting equation (2) and (3) in equation (1), rearranging gives:

$$\frac{dX}{1-X} = \frac{A}{\beta} e^{-\frac{E}{RT}}\, dT \tag{5}$$

The above equation can be used to evaluate *E* and *A* at constant heating rate using TG data. Unfortunately, the right hand side of equation (5) has no definite integral which makes it difficult to find the exact solution. Therefore, several procedures are devised to estimate the value of the temperature integral. In the following sections three different methods are discussed which can be used to evaluate the value of Arrhenius parameters using equation (5). Among these methods, two are based on the approximation of temperature integral while the third uses a differential approach commonly known as "Direct Arrhenius plot method".

4.1. INTEGRAL METHOD

This method is based on the approximation of temperature integral made by (Coats and Redfern 1964), and it is widely used and accepted for the calculation of kinetics parameters. For each discrete event of pyrolysis, equation (5) is integrated with temperature limits from T_0 to *T* while the conversion factor (*X*) has the limits 0 to *X*:

$$\int_0^X \frac{dX}{1-X} = \frac{A}{\beta} \int_{To}^{T} e^{-\frac{E}{RT}}\, dT \tag{6}$$

Integration of left side of equation (6) gives:

$$\int_0^X \frac{dX}{1-X} = -\ln(1-X) \tag{7}$$

As the right hand side of equation (6) has no definite integral, assumptions are made to solve this integral. The first assumption is to take $T_0 = 0$, as no reaction is taking place at T_0 and also *X* is zero at T_0. Therefore the right hand side of equation (6) becomes:

$$\frac{A}{\beta} \int_{To}^{T} e^{-\frac{E}{RT}}\, dT = \frac{A}{\beta} \int_{0}^{T} e^{-\frac{E}{RT}}\, dT \tag{7.a}$$

Now suppose,

$$u = \frac{E}{RT} \tag{7.b}$$

this gives,

$$\frac{A}{\beta} \int_{0}^{T} e^{-\frac{E}{RT}}\, dT = \frac{AE}{\beta R} \int_{u}^{\infty} u^{-2} e^{-u}\, du \tag{7.c}$$

A.W.Coats (Coats and Redfern 1964) has used series of expansion to solve the right hand side of the above integral which results in the following:

$$\frac{AE}{\beta R}\int_{u}^{\infty} u^{-2}e^{-u}\,du = \mathrm{T}^2\left\{\frac{AR}{\beta E}\left[1-\frac{2RT}{E}\right]\right\}e^{-\frac{E}{RT}} \tag{8}$$

Substituting equation (7) and (8) in equation (6):

$$\frac{-\ln(1-X)}{T^2} = \left\{\frac{AR}{\beta E}\left[1-\frac{2RT}{E}\right]\right\}e^{-\frac{E}{RT}} \tag{8.a}$$

Taking natural log on both sides:

$$\ln\left(\frac{-ln(1-X)}{T^2}\right) = ln\frac{AR}{\beta E}\left[1-\frac{2RT}{E}\right]-\frac{E}{RT} \tag{8.b}$$

The above equation can be more simplified by assuming$E \gg 2RT$. Which is a reasonable assumption, as the value of activation energy (*E*) is normally 5-10 order of magnitude more than the product *2RT* (at least for oil shale):

$$ln\left(-\frac{\ln(1-X)}{T^2}\right) = -\frac{E}{R\,T} + ln\frac{A\,R}{\beta\,E} \tag{9}$$

The above equation represents the equation of a straight line having a slope of $-\frac{E}{R}$ and an intercept of $ln\frac{A\,R}{\beta\,E}$. Using the values of *X* and *T* from TG experiment, a graph of left hand side of equation (9) can be plotted against $\frac{1}{T}$. The plot should result in a series of data points close to a straight line. Regression analysis with least square fitting method is used to find the equation of the straight line and plot it to evaluate the values of *E* and *A*.

4.2. DIRECT ARRHENIUS PLOT METHOD

Equation (9) can be modified by taking natural log on both sides,

$$ln\left(\frac{1}{1-X}\frac{dX}{dT}\right) = ln\frac{A}{\beta} - \frac{E}{RT} \tag{9.a}$$

Rearranging above equation,

$$ln\left(\frac{1}{1-X}\frac{dX}{dT}\right) = -\frac{E}{R}\left(\frac{1}{T}\right) + ln\frac{A}{\beta} \tag{10}$$

where

$$\frac{dX}{dT} = \frac{X_{T_2}-X_{T_1}}{T_2-T_1} \tag{10.a}$$

The value of above differential can be taken from DTG curve, as shown in Figure 4.

Putting the above value in equation (10),

$$ln\left(\frac{1}{1-X}\left(\frac{X_{T_2}-X_{T_1}}{T_2-T_1}\right)\right) = -\frac{E}{R}\left(\frac{1}{T}\right) + ln\frac{A}{\beta} \tag{11}$$

Similar to the *Integral method*, a plot of the left hand side of equation (11) is obtained and least square regression analysis is used to find *E* and *A*.

4.3. METHOD OF APPROXIMATE TEMPERATURE INTEGRAL

The temperature integral of Arrhenius equation has no definite integral as reported by many authors (Coats and Redfern 1964; Tang, Liu et al. 2003; Lapuerta, Hernandez et al. 2004; Qing, Baizhong et al. 2007). Throughout earlier research, different techniques are used to approximate the temperature integral(Obaid, Alyoubi et al. 2000; Diefallah, Gabal et al. 2001; Órfão and Martins 2002). By taking an appropriate function, an approximated value of temperature integral can be calculated for specific cases. From equation (6),

$$\int_0^X \frac{dX}{1-X} = \frac{A}{\beta}\int_0^T e^{-\frac{E}{RT}}\,dT \qquad (11.a)$$

or,

$$-\ln(1-X) = \frac{AE}{\beta R}\,P(u) \qquad (12)$$

where,

$$P(u) = \int_u^\infty u^{-2}e^{-u}\,du \qquad (12.a)$$

The above integral shows that exponential temperature integral varies with u, therefore an approximated function can be written for *P(u)* based on logarithmic change, as follows (Tang, Liu et al. 2003):

$$\ln P(u) = a + bu + clnu \qquad (13)$$

where, *P(u)* is the temperature integral and a, b and c are the coefficients. By differentiating above equation with respect to u, we get:

$$\frac{d\ln P(u)}{du} = b + \frac{c}{u} \qquad (14)$$

Plotting the left hand side of the above equation with 1/u gives a straight line and values of *b* and *c* can be calculated using the slope and intercept of the line respectively. However, u values are required for plotting the line. In fact, *u* itself depends upon *E*, which is an unknown, and also it varies with the temperature. So, a justifiable range for the value of *u* can be assumed for which equation (14) can be plotted. The easiest way is to estimate the range of *u* by referring to the literature for the specific feedstock. For oil shale, data is available from (Lapuerta, Hernandez et al. 2004). The value of *E* ranges from 33.83 kJ/mol to 66.10 kJ/mol over the temperature range of 300 K to 1100 K. These activation energy values result in a range of *u* form 7.2 to 13.5 approximately. Alternatively, an iterative method can be used for feedstokes for which activation energy estimates are not available.

Now the graph of the left hand side of equation (14) against 1/u is plotted for a definite range of u form 7.2 to 13.5, as shown in Figure 7. This gives the equation of a straight line as:

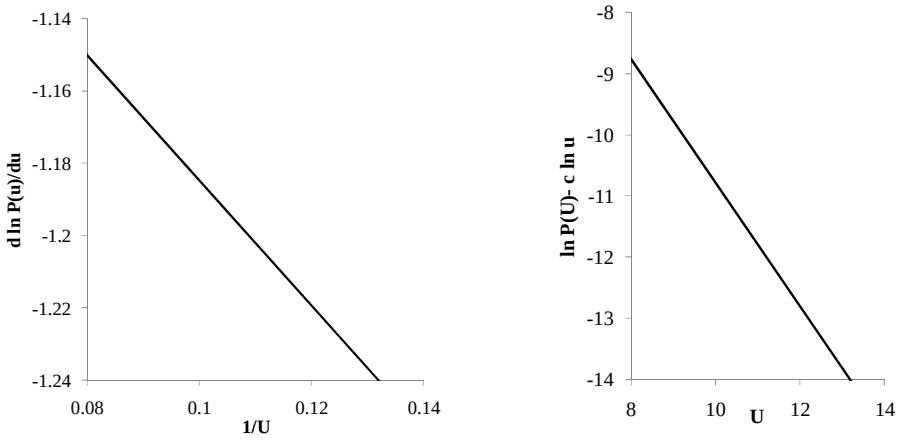

Figure 7: Plot of equation (16) (Left) and equation (18) (Right).

$$\frac{d \ln P(u)}{du} = -1.011227597 - \frac{1.734438235}{u} \quad (15)$$

By comparing equation (14) and (15) the values of *b* and *c* are found to be:

$b = -1.011227597$ & $c = -1.734438235$

Similarly, to calculate the value of a, equation (13) can be written as:

$$\ln P(u) - clnu = a + bu \quad (16)$$

The only unknown in the above equation is the coefficient *a*. By plotting the left hand side of equation (16) against *u*, a straight line is obtained as shown in Figure 7. The equation of this straight line is found to be:

$$\ln P(u) - c \ln u = -0.677458478 - 1.010814986\, u \quad (17)$$

By comparing equation (16) and (17) the value of *a* is found to be -0.677458478. Although the result for *b* is deviated in equation (17) but for an approximated result this error is acceptable.

Substituting the value of *a*, *b*, and *c* in equation (13), gives:

$$\ln P(u) = -0.677458478 - 1.011227597\, u \; - 1.734438235\, lnu \quad (18)$$

Substituting the value of equation (18) in (12), after simplification gives:

$$\ln\left(-\frac{ln(1-X)}{T^{1.734438235}}\right) = \left[ln\frac{AE}{hR} + 2.996077559 - 1.734438235\ \ln(E)\right] - 1.011227597\left(\frac{E}{R\,T}\right) \quad (19)$$

Plotting left hand side of the above equation against $\frac{1}{T}$ gives a series of data points close to a straight line. After performing least square regression data analysis an equation of a straight line is obtained. From the slope and intercept of the line, *E* and *A* can be calculated.

5. RESULTS AND DISCUSSION

Regression analysis of scattered data points generated from equation (9), (11), and (19) gives a straight line as shown in Figure 8. Where, *Y* represents the left hand side of plotted equations. Ideally, the scatter data points should represent a trend of a straight line rather than a curved one.

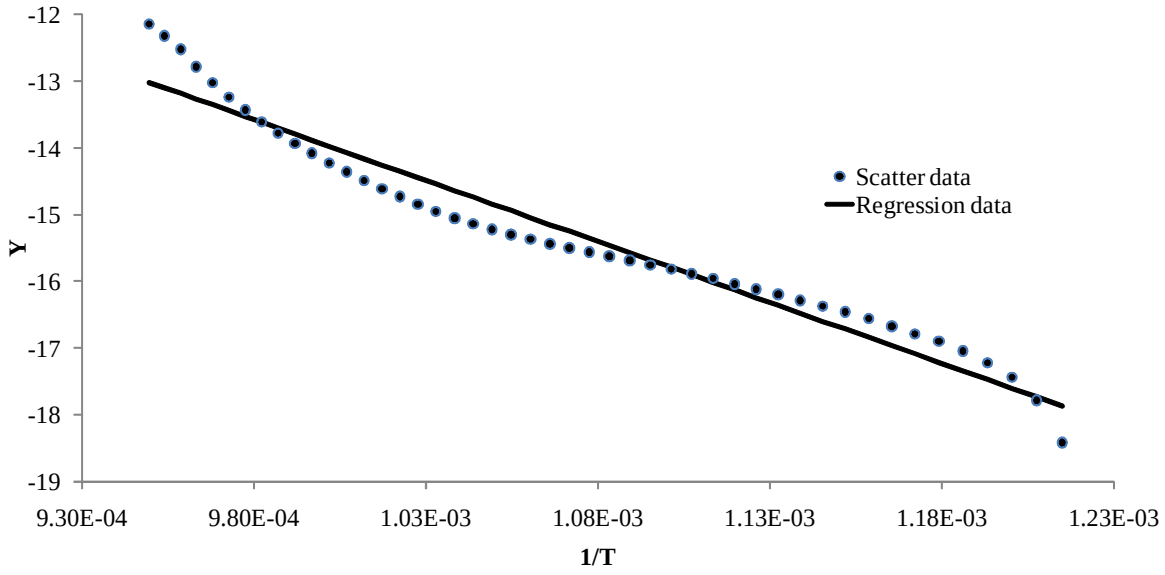

Figure 8: Arrhenius plot for devolatization from oil shale at 20°C/min.

This is because of the assumption of unity reaction order. Therefore the prior knowledge of the order of reaction is necessary otherwise; an iterative technique can be applied to determine the order of reaction. This is achieved by selecting some initial values for the order of the reaction and then plotting the TG data similarly as Figure 8. The order of reaction at which the scattered plot gives a straight line becomes the realistic order of reaction. The correlation coefficient of regression line, as plotted in Figure 8, has the value of 0.95, which shows its close similitude with the scattered data. Therefore it makes the assumption of taking order of reaction as unity reasonable accurate. From the slope and intercept of regression line, *E* and *A* can be calculated. For each event of pyrolysis of oil shale, the results of activation energy and pre-exponent factor calculated by different methods are summarized in Table 3.

Table 3: Kinetic parameters (*E* and *A*) for pyrolysis of oil shale at various heating rates.

METHODS:		INTEGRAL METHOD		DIRECT ARRHENIUS PLOT METHOD		APPROX. TEMP. INTEGRAL METHOD	
Heating Rate	Events	E (KJ/mol)	A (sec^{-1})	E (KJ/mol)	A (sec^{-1})	E (KJ/mol)	A (sec^{-1})
20 K/min	Drying	15.9	2.22E-01	8.3	3.26E-02	17.0	3.97E-01
	Devolatization	64.5	2.19E+02	60.7	1.51E+02	66.7	3.02E+02
	Boudouard	152.0	4.71E+05	172.0	7.98E+06	155.8	5.59E+05
15 K/min	Drying	5.9	4.70E-03	8.0	1.96E-02	6.9	1.16E-02
	Devolatization	65.8	2.13E+02	64.2	2.16E+02	68.0	2.92E+02
	Boudouard	173.8	8.03E+06	182.2	2.76E+07	177.8	9.18E+06
10 K/min	Drying	5.6	2.30E-03	4.7	3.90E-03	6.6	5.80E-03
	Devolatization	65.3	1.73E+02	60.5	9.66E+01	67.6	2.38E+02
	Boudouard	171.2	3.25E+06	145.3	1.16E+05	175.3	3.76E+06
5 K/min	Drying	10.9	5.80E-03	5.0	1.60E-03	11.9	1.18E-02
	Devolatization	65.8	1.17E+02	56.2	2.62E+01	68.0	1.60E+02
	Boudouard	168.1	1.61E+06	122.2	4.19E+03	172.2	1.87E+06

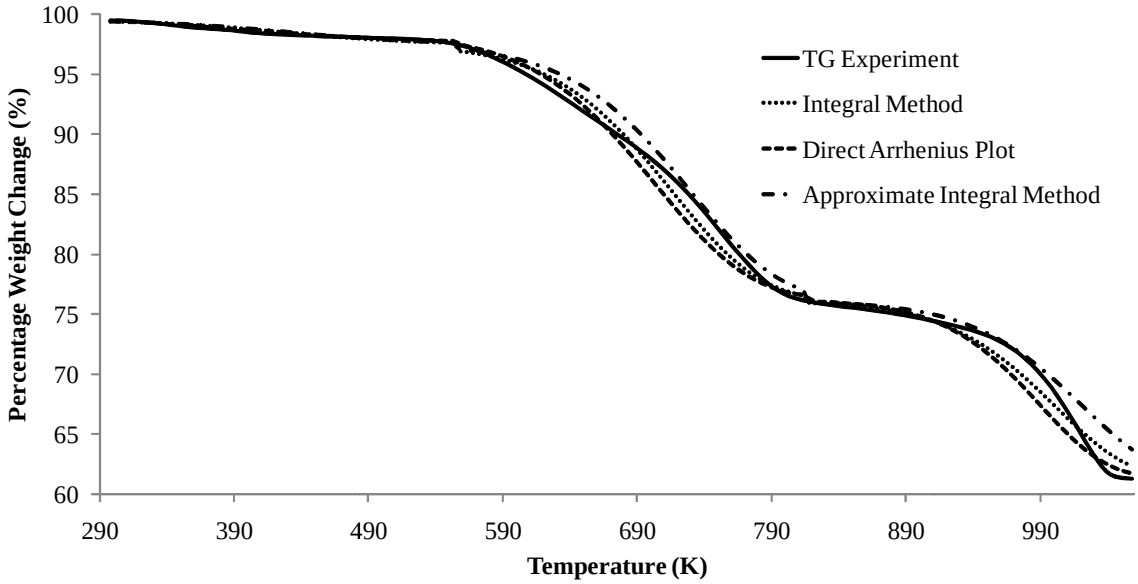

Figure 9: Comparison of TG experimental data and modeled results for 20°C/min heating rate.

For these kinetics parameters, percentage weight change of oil shale can be simulated. This can be done by substituting the values of *E* and *A* back in equation (9), (11) and (19) and then plot it to a temperature range corresponding to each event. Figure 9 shows the plot of percentage weight change for each kinetic method at 20°C/min heating rate. It shows a good agreement between the TG experimental data and modeled results. Also, root mean square error (RMSE) for three kinetics methods is calculated as shown in Table 4. The result of RMSE for integral method is found to be less than that of other two kinetic methods for all heating rates which makes the overall results of integral method closer to TG experimental data as compared to other methods.

Table 4: Results of root mean square error (RMSE) for each kinetic method

METHODS	INTEGRAL METHOD	DIRECT ARRHENIUS PLOT METHOD	APPROX. TEMP. INTEGRAL METHOD
Heating Rate	RMSE	RMSE	RMSE
20 K/min	0.71	1.01	1.04
15 K/min	0.63	0.94	0.91
10 K/min	0.54	0.80	1.04
5 K/min	0.57	0.89	1.35

6. CONCLUSIONS:

Thermogravimetric (TG) analysis data of the oil shale obtained at MI are studied to evaluate the kinetics parameters for pyrolysis of El-Lujjun oil shale. Four different heating rates are used for the pyrolysis with constant flow rate of nitrogen. Above 600°C, char undergoes Boudouard reaction with

CO_2, forming CO. The comparison of the TG results of pyrolysis with oxidation shows that the amount of CO_2 evolving is enough to consume char and hence the Boudouard reaction can be modeled as a first order independent of CO_2. Comparing the TG results for pyrolyzed and/or combusted oil shale with those of its ultimate analysis proved the existence of sulfur in ash that is not easily reacted under TG conditions. Finally, kinetic behavior of pyrolysis of oil shale is studied. The calculated kinetic parameters results are compared with the experimental curve of TG analysis and also among themselves. A Root mean square error is calculated for each method and the Integral method model was found to be the closest to experimental data.

7. REFERENCES

Bockhorn, H., A. Hornung, et al. (1999). "Mechanisms and kinetics of thermal decomposition of plastics from isothermal and dynamic measurements." Journal of Analytical and Applied Pyrolysis 50(2): 77-101.

Capart, R., L. Khezami, et al. (2004). "Assessment of various kinetic models for the pyrolysis of a microgranular cellulose." Thermochimica Acta 417(1): 79-89.

Choi, Y. C., X. Y. Li, et al. (2001). "Numerical study on the coal gasification characteristics in an entrained flow coal gasifier." Fuel 80(15): 2193-2201.

Coats, A. and J. Redfern (1964). "Kinetic parameters from thermogravimetric data."

Diefallah, E., M. Gabal, et al. (2001). "Nonisothermal decomposition of CdC2O4-FeC2O4 mixtures in air." Thermochimica Acta 376(1): 43-50.

Dogan, Ö. M. and B. Z. Uysal (1996). "Non-isothermal pyrolysis kinetics of three Turkish oil shales." Fuel 75(12): 1424-1428.

Dollimore, D., T. A. Evans, et al. (1992). "Correlation between the shape of a TG/DTG curve and the form of the kinetic mechanism which is applying." Thermochimica Acta 198(2): 249-257.

Dyni, R. J. "Geology and Resources of Some World Oil Shale Deposits: Scientific Investigations Report 2005- 5294, US Department of the Interior; available online at: htpp://www.usgs.gov/sir/2006/5394.

Jaber, J. and S. Probert (1999). "Pyrolysis and gasification kinetics of Jordanian oil-shales." Applied Energy 63(4): 269-286.

Kök, M. V. and M. R. Pamir (2000). "Comparative pyrolysis and combustion kinetics of oil shales." Journal of Analytical and Applied Pyrolysis 55(2): 185-194.

Lapuerta, M., J. Hernandez, et al. (2004). "Kinetics of devolatilisation of forestry wastes from thermogravimetric analysis." Biomass and bioenergy 27(4): 385-391.

Leung, D. Y. C. and C. L. Wang (1998). "Kinetic study of scrap tyre pyrolysis and combustion." Journal of Analytical and Applied Pyrolysis 45(2): 153-169.

Liu, N. A., W. Fan, et al. (2002). "Kinetic modeling of thermal decomposition of natural cellulosic materials in air atmosphere." Journal of Analytical and Applied Pyrolysis 63(2): 303-325.

Madhusudanan, P. M., K. Krishnan, et al. (1986). "New approximation for the p(x) function in the evaluation of non-isothermal kinetic data." Thermochimica Acta 97: 189-201.

Obaid, A., A. Alyoubi, et al. (2000). "Kinetics of thermal decomposition of copper (II) acetate monohydrate." Journal of Thermal Analysis and Calorimetry 61(3): 985-994.

Oja, V., A. Elenurm, et al. (2007). "Comparison of oil shales from different deposits: oil shale pyrolysis and co-pyrolysis with ash." Oil Shale 24(2): 101.

Órfão, J. and F. Martins (2002). "Kinetic analysis of thermogravimetric data obtained under linear temperature programming--a method based on calculations of the temperature integral by interpolation* 1." Thermochimica Acta 390(1-2): 195-211.

Q.Rana, T. I., S.Shabbar,J. Isam, H.Mohammed (2010). "Material Characterization and Gasification of Jordanian Oil Shale." International Journal of Energy, Environment, and Ecomomics(Accepted for publication).

Qing, W., S. Baizhong, et al. (2007). "Pyrolysis characteristics of Huadian oil shales." Oil Shale 24(2): 147.

Rajeshwar, K. (1981). "The kinetics of the thermal decomposition of green river oil shale kerogen by non-isothermal thermogravimetry." Thermochimica Acta 45(3): 253-263.

Rao, T. R. and A. Sharma (1998). "Pyrolysis rates of biomass materials." Energy 23(11): 973-978.

Shawabkeh, R., A. Al-Harahsheh, et al. (2004). "Copper and zinc sorption by treated oil shale ash." Separation and Purification Technology 40(3): 251-257.

Shawabkeh, R. and A. Harahsheh (2007). "H~ 2S removal from sour liquefied petroleum gas using Jordanian oil shale ash." Oil Shale 24(2): 109.

Starink, M. J. (2003). "The determination of activation energy from linear heating rate experiments: a comparison of the accuracy of isoconversion methods." Thermochimica Acta 404(1-2): 163-176.

Strizhakova, Y. and T. Usova (2008). "Current trends in the pyrolysis of oil shale: A review." Solid Fuel Chemistry 42(4): 197-201.

Tang, W., Y. Liu, et al. (2003). "New approximate formula for Arrhenius temperature integral." Thermochimica Acta 408(1-2): 39-43.

Thakur, D. and H. Nuttall Jr (1987). "Kinetics of pyrolysis of Moroccan oil shale by thermogravimetry." Industrial & Engineering Chemistry Research 26(7): 1351-1356.

Vyazovkin, S. and C. A. Wight (1999). "Model-free and model-fitting approaches to kinetic analysis of isothermal and nonisothermal data." Thermochimica Acta 340-341: 53-68.

Watanabe, H. and M. Otaka (2006). "Numerical simulation of coal gasification in entrained flow coal gasifier." Fuel 85(12-13): 1935-1943.

Williams, P. T. and N. Ahmad (2000). "Investigation of oil-shale pyrolysis processing conditions using thermogravimetric analysis." Applied Energy 66(2): 113-133.

Yu, L., J. Lu, et al. "Numerical simulation of the bubbling fluidized bed coal gasification by the kinetic theory of granular flow (KTGF)." Fuel 86(5-6): 722-734.